SUPPLEMENTAL MATERIAL

SUPPLEMENTAL METHODS

Materials and reagents. Tissue culture dishes and Permanox® chamberslides were from Nunc (Naperville, IL). Dulbecco's Modified Eagle Medium (DMEM) was from Life Technologies (Grand Island, NY). Heat-inactivated fetal bovine serum (FBS) was from Hyclone Laboratories (Logan, UT). Rabbit anti-FAK (pY397), anti-FAK (pY861), anti-FAK (pY925), anti-paxillin (pY118), and anti-PYK2 (pY402) phosphospecific rabbit polyclonal antibodies (pAb) were from BioSource International (Camarillo, CA). Phospho-ERK1/2 pAb (pT183/pY185) was from Promega (Madison, WI). $p130^{Cas}$ mouse monoclonal antibody (mAb) for immunoprecipitation was from Millipore (Billerica, MA); phospho-$p130^{Cas}$ (pY165) pAb for Western blotting was from Cell Signaling (Danvers, MA), and rabbit $p130^{Cas}$ pAb for immunocytochemistry was from Santa Cruz (Santa Cruz, CA). Anti-GFP mAb was from Stressgen (Ann Arbor, MI). Anti-paxillin, anti-PYK2, and anti-N-terminal FAK mAb were from BD Transduction Laboratories (Lexington, KY). Anti-GAPDH mAb was purchased from Novus Biologicals (Littleton, CO). Horseradish peroxidase-conjugated goat anti-rabbit and anti-mouse IgG were from BioRad (Hercules, CA). Rhodamine-conjugated goat anti-rabbit and anti-mouse IgG were obtained from Invitrogen (Carlsbad, CA). Rainbow molecular weight standards were from Amersham (Arlington Heights, IL). Pico-West and LumiGLO Enhanced Chemiluminescence (ECL) kits were from Thermo-Scientific (Hudson, NH) and KPL (Gaithersburg, MD), respectively. Costar transwell polystyrene plates were from Corning Costar (Cambridge, MA). PF573,228 was obtained from Tocris Bioscience (Ellisville, MO). PP2 and PP3 were from EMD Chemicals (Gibbstown, NJ). All other reagents were of the highest grade commercially available and were obtained from Sigma Chemical (St. Louis, MO).

Cell culture. Rat aortic smooth muscle cells (RASMCs) were isolated as previously described[1] and maintained in DMEM containing 10% FBS. Cells up to the 9th passage were used.

Adenoviral constructs. Wildtype (wt) chick FRNK was kindly provided by Dr. Tom Parsons, University of Virginia, and cloned in-frame into pEGFP expression plasmid (Clontech, Palo Alto, CA) as previously described.[2] Mutagenesis of the GFP-wtFRNK expression plasmid was then performed using the Stratagene QuikChange Kit (Stratagene, La Jolla, CA). Two sets of 35mer oligo primers were used to generate the desired mutations (Y168F, Y232F, and Y168,232F mutations, respectively) which were confirmed by DNA sequencing. Replication-defective adenoviruses (Adv) expressing GFP, GFP-wtFRNK, GFP-Y168F-FRNK, GFP-Y232F-FRNK, and GFP-Y168,232F-FRNK were then generated using the AdEasy XL system (Agilent Technologies, Santa Clara, CA), amplified, and purified as previously described.[2]

Two replication-deficient Adv expressing shRNAs specific for rat FAK[3,4] and PYK2[5] were also generated. The siRNA sequences were designed using GenScript siRNA Construct Builder. Each siRNA sequence had a MluI site at the 5' end, and a HindIII site at the 3' end. Sequences for each different target gene are shown in Supplemental Table I. The oligos were PAGE-purified and dissolved in H_2O to a concentration of 1μg/μl. Top and bottom oligos (1μg) were mixed in annealing buffer (1xSSC) and boiled at 95°C for 10 min. The mixture was then incubated at room temperature for 1h and diluted to a final concentration of 40ng/μl. The annealed oligos were then subcloned into pRNAT-H1.1/Adeno shuttle vector (GeneScript, Piscataway, NJ) for use with the AdEasy Adenoviral XL Vector System. The cloning results were confirmed by DNA sequencing. An Adv expressing shRNA specific for luciferase (Adv-Luci-shRNA) was similarly generated, and used to control for nonspecific effects of Adv infection in the gene silencing experiments.[6]

A replication-deficient Adv expressing GFP-CRNK was generated by PCR-cloning rat CRNK[7] from rat PYK2 cDNA, which was kindly provided by Dr. T. Sasaki, Sapporo Medical

University School of Medicine, Sapporo, Japan. The PCR product was ligated in frame into pEGFP expression plasmid, verified by DNA sequencing, and the GFP-CRNK cDNA was then subcloned into the AdEasy XL pShuttle vector for preparation of Adv-GFP-CRNK. A replication-defective Adv expressing CD2-FAK[8] was constructed using human CD2-FAK cDNA, kindly provided by Dr. Steve Nadler, Bristol-Myers Squibb Co, Princeton, NJ. Replication-deficient Adv expressing wt-p130^{Cas} (wtCas) and a nonphosphorylatable mutant of p130^{Cas} (i.e., Cas-ΔSD)[9] were kindly provided by Dr. Jody Martin, Loyola University Medical Center, Maywood, IL. In some experiments, an Adv expressing nuclear-encoded ß-galactosidase (neßgal) was also used to control for nonspecific effects of Adv infection.

For all Adv, the multiplicity of viral infection (moi) was determined by dilution assay in HEK293 cells grown in 96 well clusters. RASMCs were growth-arrested in serum-free culture medium for at least 1h prior to infection. Cells were incubated (24h, 37^{o}C) with Adv in serum-free medium, and the medium was replaced with serum-free DMEM for an additional 24-96h.

Immunoprecipitation, co-immunoprecipitation, SDS-PAGE and Western blotting. For Western blotting experiments, cells were homogenized in lysis buffer[10] and protein concentration was determined by bicinchoninic acid protein assay (Pierce Chemical Co., Rockford IL) using bovine serum albumin as standard. Equal amounts of extracted proteins (50µg) were directly separated by SDS-PAGE on 10% gels. Separated proteins were transferred to nitrocellulose, and the membranes were probed with the appropriate phosphospecific and total antibodies. Primary antibody binding was detected with horseradish peroxidase-conjugated goat anti-rabbit or anti-mouse secondary antibody, and visualized by ECL. Band intensity was quantified using an HP Scanjet 4890 flatbed scanner and UN-SCAN-IT Gel, Ver. 6.1 software. The ratios of phosphospecific to total FAK, PYK2, p130^{Cas}, and GFP-FRNK were analyzed. In some experiments, equal loading was confirmed by quantifying GAPDH in each sample.

For immunoprecipitation experiments, cells were homogenized in lysis buffer and equal amounts of extracted proteins (1000μg) were incubated (18h, 4°C) with anti-$p130^{Cas}$ mAb. Immune complexes were recovered by adding protein A/G beads (2h, 4°C) followed by centrifugation (10,000g; 10min). The complexes were then washed, resuspended in electrophoresis sample buffer, and separated by SDS-PAGE and Western blotting.

For co-immunoprecipitation experiments, cells were scraped in homogenization buffer (25mM HEPES, pH 7.4, containing 150mM NaCl, 1.5mM $MgCl_2$, 1mM EDTA, 10mM sodium pyrophosphate, 10mM NaF, 0.1mM sodium orthovanadate, 0.5% Nonidet P-40, and 1% sodium deoxycholate). Following centrifugation (10,000g, 20 min), equal amounts of extracted cellular proteins (500-1000μg) were co-immunoprecipitated with either nonimmune IgG, anti-paxillin mAb or anti-$p130^{Cas}$ mAb overnight at 4°C followed by the addition of protein A/G beads (4h, 4°C) and centrifugation (10,000g; 10min). The complexes were then washed, resuspended in electrophoresis sample buffer, and separated by SDS-PAGE and Western blotting.

Carotid artery balloon injury. Balloon injury of the right common carotid artery was accomplished using a 2.5F double-lumen balloon catheter (NuMED, Inc., Hopkinton, NY), by a modification[11] of the method of Clowes et al.[12] Briefly, adult male Sprague-Dawley rats (~400g) were anesthetized, and the right common and external carotid arteries were surgically exposed. The external carotid artery was proximally ligated, the catheter was introduced through an arteriotomy, and advanced into the common carotid artery. The balloon was inflated to 4 atm for 1min to rupture the internal elastic lamina. The catheter was then drawn backwards and forwards three times to denude the endothelial cell layer. In some experiments, replication-deficient adenoviruses (Adv) expressing GFP or GFP-wtFRNK (~10^{10} pfu in 0.1ml) were introduced via the central lumen of the catheter and incubated for 30min. Then, the catheter was removed and the external carotid artery ligated distal to the arteriotomy site. This procedure ensured that blood flow was maintained through the common, to the internal carotid artery. One

or 2wks later, rats were re-anesthetized, and the injured and contralateral control arteries were removed. The arteries were homogenized in lysis buffer[10] for analysis of protein expression and phosphorylation by Western blotting.

RASMC invasion assay. Matrigel transwell invasion assays were performed as previously described.[13] Briefly, equal numbers of Adv-infected cells were suspended in serum-free medium, and placed in the upper chamber of Matrigel-coated Boyden chambers. AngII (100nM) was placed in the lower chamber. Cells were allowed to migrate for 2h, and cells expressing GFP, wildtype and mutant GFP-FRNK, GFP-CRNK, or FAK, PYK2 and Luciferase shRNAs were detected by fluorescence microscopy and counted using the multi-wavelength cell scoring application of Metamorph (Molecular Devices Corp., Downingtown, PA), which identifies objects on the basis of brightness and size. For all samples, the minimum brightness criterion was set to 50 counts above local background, and the maximum and minimum object diameter criteria were set to 20 and 5 pixels, respectively. For this magnification (10X objective), image scale is 1.60 μm/pixel.

Total internal reflection fluorescence (TIRF)-microscopy and fluorescence recovery after photobleaching (FRAP). RASMCs grown on 1mm glass coverslips were infected (24h, 100moi) with Adv-GFP-wtFRNK, Adv-GFP-Y168F-FRNK, Adv-GFP-Y232F-FRNK or Adv-GFP-Y168,232F-FRNK. Cells were then viewed under an inverted TIRF-microscope. TIRF-illumination was performed by a 445nm diode laser and/or multiline 300mW Argon laser via a Nikon TIRF II illuminator coupled with a custom beam combiner launch. For FRAP, the Argon laser was directed to the sample with a 10/90 beam splitter mounted in a second filter cube carousel positioned above the excitation dichroic. Bleach spot sizing was accomplished with a Keplerian telescope mounted on an XYZ translation stage. Laser routing and photobleaching exposure time were controlled by Uniblitz shutters driven with a shutter/filter wheel controller

interfaced to a computer. A single peripheral FA in an individual cell (20 cells per group) was randomly selected, and subjected to FRAP analysis. Fluorescence intensity data were acquired every 22.9 msec for up to 20 sec after photobleaching a small region of interest encompassing a single FA site. Fluorescence intensity data immediately after the laser flash (F) were then normalized to the initial fluorescence intensity (F_0) and plotted as a function of time (sec). Data were then fit to the following double-exponential function:

$$F/F_0 = Y_0 + M1*(1-e^{k1*t}) + M2*(1-e^{k2*t})$$

where Y_0 was the best-fitting value for F/F_0 at t=0 (i.e., immediately after the flash), M1 and M2 were the fraction of total fluorescence in the "fast" and "slow" compartments, respectively, and k1 and k2 were the first-order rate constants (sec^{-1}) describing the rate of rise of F/F_0 in each of the two compartments. Unweighted data were fit using SigmaStat Ver. 3.1 software. Best-fitting values for M1, k1, M2 and k2 were then used to calculate a single "average" rate constant for each cell (k_{FRAP}, sec^{-1}) describing the rate of rise of F/F_0 to plateau:

$$\text{Average } k_{FRAP} = M1*k1 + M2*k2$$

Cell fixation and confocal microscopy. RASMCs grown on Permanox® chamberslides were infected with Adv expressing GFP, GFP-wtFRNK and GFP-Y168F-FRNK (100 moi, 24h) Cells were fixed in 2% paraformaldehyde in PBS, permeabilized with 1% Triton X-100 in PBS, and stained with anti-$p130^{Cas}$ or anti-paxillin antibodies. Fluorescently labeled cells were viewed with a Leica TCS SP5 laser scanning confocal microscope.

Statistical analysis. Results were expressed as means±SEM. Data for multiple groups were compared by 2-ANOVA followed by the Holm-Sidak test, and 1-way ANOVA or 1-way ANOVA on Ranks followed by the Student-Newman-Keuls test. Data for 2 groups were compared by unpaired t-test or Mann-Whitney Rank Sum test, where appropriate. Differences among means were considered significant at $P<0.05$. Data were analyzed using the SigmaStat Statistical Software Package, Ver. 3.1 (Systat Software, San Jose, CA).

SUPPLEMENTAL REFERENCES

1. Sabri A, Govindarajan G, Griffin TM, Byron KL, Samarel AM, Lucchesi PA. Calcium- and protein kinase C-dependent activation of the tyrosine kinase PYK2 by angiotensin II in vascular smooth muscle. *Circ Res* 1998;83:841-851.
2. Heidkamp MC, Bayer AL, Kalina JA, Eble DM, Samarel AM. GFP-FRNK disrupts focal adhesions and induces anoikis in neonatal rat ventricular myocytes. *Circ Res* 2002;90:1282-1289.
3. Tilghman RW, Slack-Davis JK, Sergina N, Martin KH, Iwanicki M, Hershey ED, Beggs HE, Reichardt LF, Parsons JT. Focal adhesion kinase is required for the spatial organization of the leading edge in migrating cells. *J Cell Sci* 2005;118:2613-2623.
4. Mon NN, Hasegawa H, Thant AA, Huang P, Tanimura Y, Senga T, Hamaguchi M. A role for focal adhesion kinase signaling in tumor necrosis factor-α-dependent matrix metalloproteinase-9 production in a cholangiocarcinoma cell line, CCKS1. *Cancer Res* 2006;66:6778-6784.
5. Sayas CL, Ariaens A, Ponsioen B, Moolenaar WH. GSK-3 is activated by the tyrosine kinase Pyk2 during LPA1-mediated neurite retraction. *Mol Biol Cell* 2006;17:1834-1844.

6. Ohtsuka T, Ryu H, Minamishima YA, Macip S, Sagara J, Nakayama KI, Aaronson SA, Lee SW. ASC is a Bax adaptor and regulates the p53-Bax mitochondrial apoptosis pathway. *Nat Cell Biol* 2004;6:121-128.

7. Li X, Dy RC, Cance WG, Graves LM, Earp HS. Interactions between two cytoskeleton-associated tyrosine kinases: calcium-dependent tyrosine kinase and focal adhesion tyrosine kinase. *J Biol Chem* 1999;274:8917-8924.

8. Chan PY, Kanner SB, Whitney G, Aruffo A. A transmembrane-anchored chimeric focal adhesion kinase is constitutively activated and phosphorylated at tyrosine residues identical to $pp125^{FAK}$. *J Biol Chem* 1994;269:20567-20574.

9. Kovacic-Milivojevic B, Roediger F, Almeida EA, Damsky CH, Gardner DG, Ilic D. Focal adhesion kinase and $p130^{Cas}$ mediate both sarcomeric organization and activation of genes associated with cardiac myocyte hypertrophy. *Mol Biol Cell* 2001;12:2290-2307.

10. Schlaepfer DD, Hunter T. Evidence for in vivo phosphorylation of the Grb2 SH2-domain binding site on focal adhesion kinase by Src-family protein-tyrosine kinases. *Mol Cell Biol* 1996;16:5623-5633.

11. Koshman YE, Engman SJ, Kim T, Iyengar R, Henderson KK, Samarel AM. Role of FRNK tyrosine phosphorylation in vascular smooth muscle spreading and migration. *Cardiovasc Res* 2010;85:571-581.

12. Clowes AW, Reidy MA, Clowes MM. Kinetics of cellular proliferation after arterial injury. I. Smooth muscle growth in the absence of endothelium. *Lab Invest* 1983;49:327-333.

13. Koshman YE, Kim T, Chu M, Engman SJ, Iyengar R, Robia SL, Samarel AM. FRNK inhibition of focal adhesion kinase-dependent signaling and migration in vascular smooth muscle cells. *Arterioscler Thromb Vasc Biol* 2010;30:2226-2233.

SUPPLEMENTAL FIGURE LEGENDS

Supplemental Figure I. *FRNK inhibits VSMC FAK and PYK2 phosphorylation and cell invasion.* Rat aortic smooth muscle cells (RASMCs) were infected (100moi, 24h) with Adv-GFP or Adv-GFP-wtFRNK. Paired cultures were then stimulated with AngII (100nM; 30min). (A) FAK-Y397, FAK-Y861 and FAK-Y925 phosphorylations were analyzed by Western blotting with phosphospecific antibodies. An N-terminal FAK antibody was used to ensure equal loading. (B) FRNK-Y168 and FRNK-Y232 phosphorylations were analyzed by Western blotting with the same phosphospecific antibodies. GFP and GAPDH antibodies were used to ensure equal loading. (C) PYK2-Y402 phosphorylation was analyzed by Western blotting, and a C-terminal PYK2 antibody was used to ensure equal loading. The position of molecular weight markers is indicated to the left of each blot. (D) Equal numbers of Adv-infected cells (100moi, 24h) were suspended in serum-free medium, and placed in the upper chamber of Matrigel-coated Boyden chambers. AngII (100nM) was placed in the lower chamber. Cells were allowed to migrate for 2h, and cells expressing GFP or GFP-FRNK were detected by fluorescence microscopy and counted using an automatic cell scoring application. Representative object scoring maps from a single experiment are depicted.

Supplemental Figure II. *Effects of GFP-wtFRNK and GFP-wtCRNK overexpression on VSMC invasion.* RASMCs were infected (100moi, 24h) with Adv-GFP, Adv-GFP-wtFRNK, or Adv-GFP-wtCRNK. Equal numbers of Adv-infected cells were suspended in serum-free medium, and placed in the upper chamber of Matrigel-coated Boyden chambers. AngII (100nM) was placed in the lower chamber. Cells were allowed to migrate for 2h, and cells expressing GFP, GFP-wtFRNK or GFP-wtCRNK were detected by fluorescence microscopy and counted using an automatic cell scoring application. (A) Representative object scoring maps from a single

experiment are depicted. (B) Quantitative analysis of 20 images per group from 3 separate experiments were analyzed. Data are mean±SEM; *P<0.05 *vs.* GFP; $^{\#}P$<0.05 vs. GFP-wtFRNK.

Supplemental Figure III. *FAK tyrosine phosphorylation at Y861 and Y925 is critical for VSMC invasion*. (A) Paired cultures were stimulated with AngII (100nmol/L, 10min) in the absence or presence of PF (100mM, 1 hr pre-treatment) , PP2 or PP3 (20μM, 1h pre-treatment). FAK Y397, Y861 and Y925 phosphorylation were analyzed by Western blotting with phosphospecific antibodies. (B) Paired cultures were stimulated with AngII (100nmol/L, 30min) in the absence or presence of PF, PP2 or PP3 (20μM, 1h pre-treatment). FAK Y397, Y861 and Y925 phosphorylation were analyzed by Western blotting with phosphospecific antibodies. (C) Equal numbers of Adv-infected cells were suspended in serum-free medium, and placed in the upper chamber of Matrigel-coated Boyden chambers. AngII (100nmol/L) was placed in the lower chamber, in the absence or presence of PF (100mM, 1 hr pre-treatment) or PP2 or PP3 (20μM, 1h pre-treatment) (D). Cells were allowed to migrate for 2h, and fluorescently labeled cells were visualized and counted. (C-D) Representative fluorescent images from a single experiment. (E) Quantitative analysis of 20 images per group from 3 separate experiments. Data are mean±SEM; *P<0.05 UT *vs* PF. (F) Quantitative analysis of 20 images per group from 3 separate experiments. Data are mean±SEM; *P<0.05 PP2 *vs* UT or PP3.

Supplemental Figure IV. *FRNK tyrosine phosphorylation is not required for efficient FA targeting and inhibition of certain aspects of FAK-dependent signaling.* (A) Live TIRF microscopic images of RASMCs infected (100moi, 24h) with Adv expressing GFP-tagged wt, Y168F-, Y232F- or Y168,232F-FRNK. (B) Tyrosine phosphorylation of endogenous FAK was analyzed by Western blotting in RASMCs infected (100moi, 24h) with Adv expressing GFP, or GFP-tagged wt, Y168F-, Y232F-, or Y168,232F-FRNK. Paired cultures were stimulated with AngII (100nM, 30min). FAK-Y397, FAK-Y861 and FAK-Y925 phosphorylations were analyzed

by Western blotting with phosphospecific antibodies, and with N-terminal FAK antibody. Pax-Y118 and ERK1/2 phosphorylations were also analyzed by Western blotting with phosphospecific antibodies. Samples were probed for GAPDH to ensure equal loading. The position of molecular weight markers is indicated to the left of each blot. (C-E) Quantitative analysis of FAK-Y397, FAK-Y861 and FAK-Y925 phosphorylations from n=4 experiments. Data are means±SEM; **P*<0.05 vs. GFP.

Supplemental Figure V. *TIRF-microscopy and FRAP analysis of wtFRNK and FRNK phosphorylation mutants.* Representative images of the recovery of GFP fluorescence at 0, 0.5, 1.0 and 5.0 sec after photobleaching are depicted for wtFRNK, Y168F-FRNK, Y232F-FRNK and Y168,232F-FRNK. The dashed circle represents the region of interest from which the quantitative analysis of GFP fluorescence recovery was obtained.

Supplemental Figure VI. *$p130^{Cas}$ and paxillin co-localize with GFP-wtFRNK and GFP-Y168-FRNK in spreading VSMCs.* RASMCs were infected (100moi, 24h) with Adv-GFP-wtFRNK or Adv-Y168F-FRNK (green). Cells were then trypsinized, replated onto fibronectin-coated chamber slides, and allowed to attach and spread at 37^{o}C for 60min. Cells were then fixed, permeabilized, counterstained with anti-$p130^{Cas}$ mAb (red; Panel A), or anti-paxillin mAb (red; Panel B), mounted with DAPI-containing mounting medium to detect cell nuclei (blue), and viewed by confocal microscopy. Co-localization of GFP fluorescence and $p130^{Cas}$ or paxillin in these 1μm optical sections at the cell-substratum interface was represented in the merged image (yellow). The bar indicates 10μm.

Supplemental Figure VII. *$pY165p130^{Cas}$ phosphorylation is Src-dependent.* (A) RASMCs were infected (100moi, 24h) with Adv-GFP, Adv-GFP-wtFRNK and Adv-Y168F-FRNK. Paired cultures were then stimulated with AngII (100 nM; 30min) in the absence or presence of PP2

(20μM, 1h pre-treatment). p130^{Cas}-Y165 phosphorylation was analyzed by Western blotting with phosphospecific antibody. (B) Model mechanism of FRNK-mediated inhibition of VSMC invasion. (Left Panel) With little or no FRNK, VSMCs migrate as a result of FAK transphosphorylation at Y397, Src-dependent FAK phosphorylation at Y861, and binding and subsequent phosphorylation of p130^{Cas} by the FAK/Src complex. (Right Panel) With wtFRNK overexpression, FRNK undergoes Src-dependent Y168 phosphorylation, targets to FAs, and subsequently binds to p130^{Cas}, but since FRNK lacks the kinase domain and Y397 autophosphorylation site present in full-length FAK, it fails to form an equivalent FRNK/Src complex which is required for p130^{Cas} phosphorylation and initiation of cell invasion.

Supplemental Table I. shRNA sequences for FAK and PYK2

Gene	Sequence
FAK-1^{Top}	5'- ***CGCG***CGCAATGGAACGAGTATTAAA***TTCAAGAGA***TTTAATACTCGTTCCATTGCATTTTTTGGAA-3'
FAK-1^{bottom}	5'- ***AGCT***TTTCCAAAAAATGCAATGGAACGAGTATTAAA***TCTCTTGAA***TTTAATACTCGTTTCCATTGCG-3'
FAK-2^{Top}	5'- ***CGCG***CGCCACCTGGGCCAGTATTAT***TTCAAGAGA***ATAATACTGGCCCAGGTGGTTTTTTGGAAA-3'
FAK-2^{bottom}	5'- ***AGCT***TTTCCAAAAAACCACCTGGGCCAGTATTAT***TCTCTTGAA***ATAATACTGGCCCAGGTGGCG-3'
PYK2-1^{Top}	5'- ***CGCG***GATGTAGTTCTTAACCGCA***TTCAAGAGA***TGCGGTTAAGAACTACATCTTTTTT-3'
PYK2-1^{bottom}	5'- ***AGCT***AAAAAAGATGTAGTTCTTAACCGCA***TCTCTTGAA***TGCGGTTAAGAACTACATC-3'
PYK-2^{Top}	5'- ***CGCG***GATGCTTGGACCCGATGGT***TTCAAGAGA***ACCATCGGGTCCAAGCATCTTTTTT-3'
PYK2-2^{bottom}	5'- ***AGCT***AAAAAAGATGCTTGGACCCGATGGT***TCTCTTGAA***ACCATCGGGTCCAAGCATC-3'

Supplemental Figure I

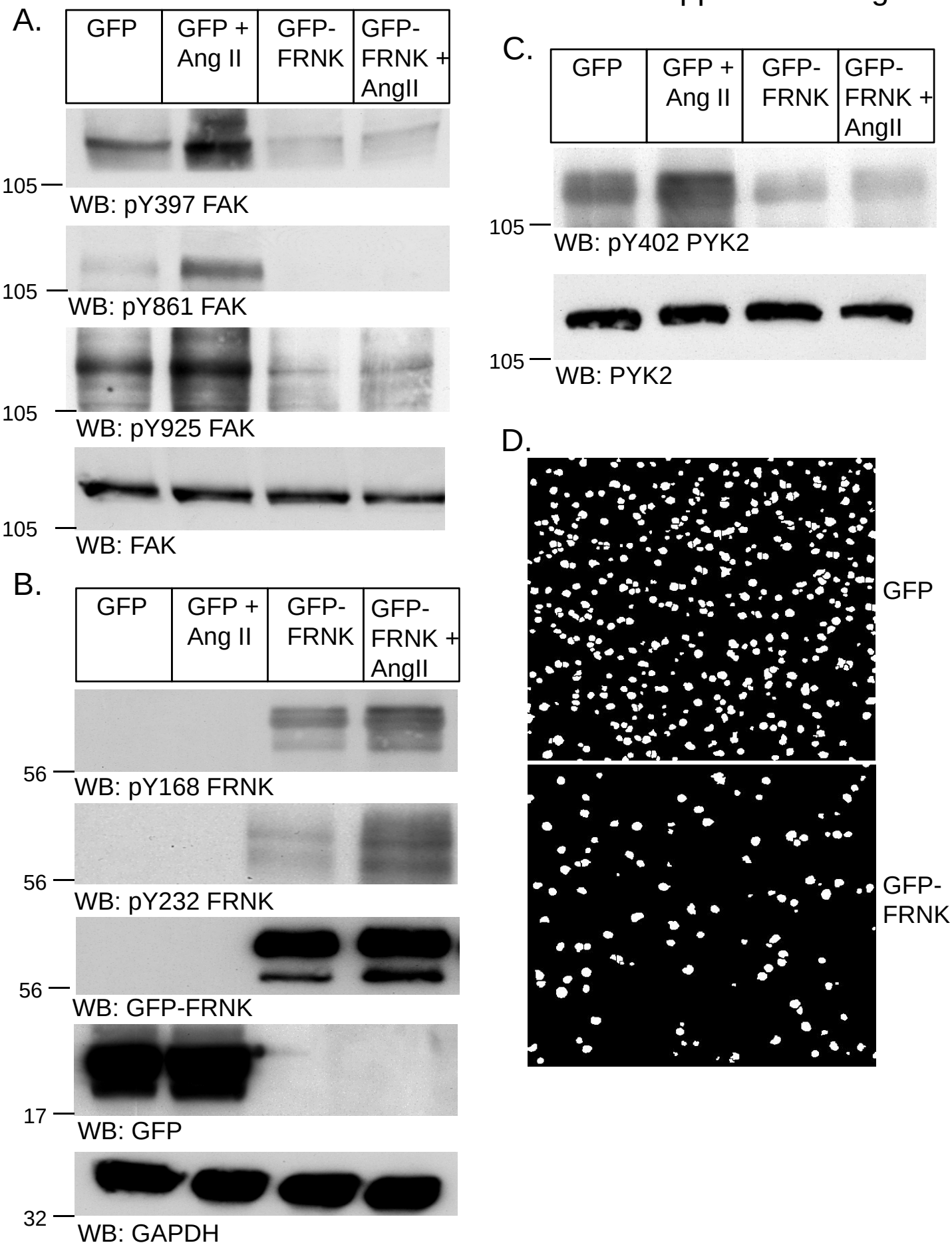

Supplemental Figure II

A.

B.

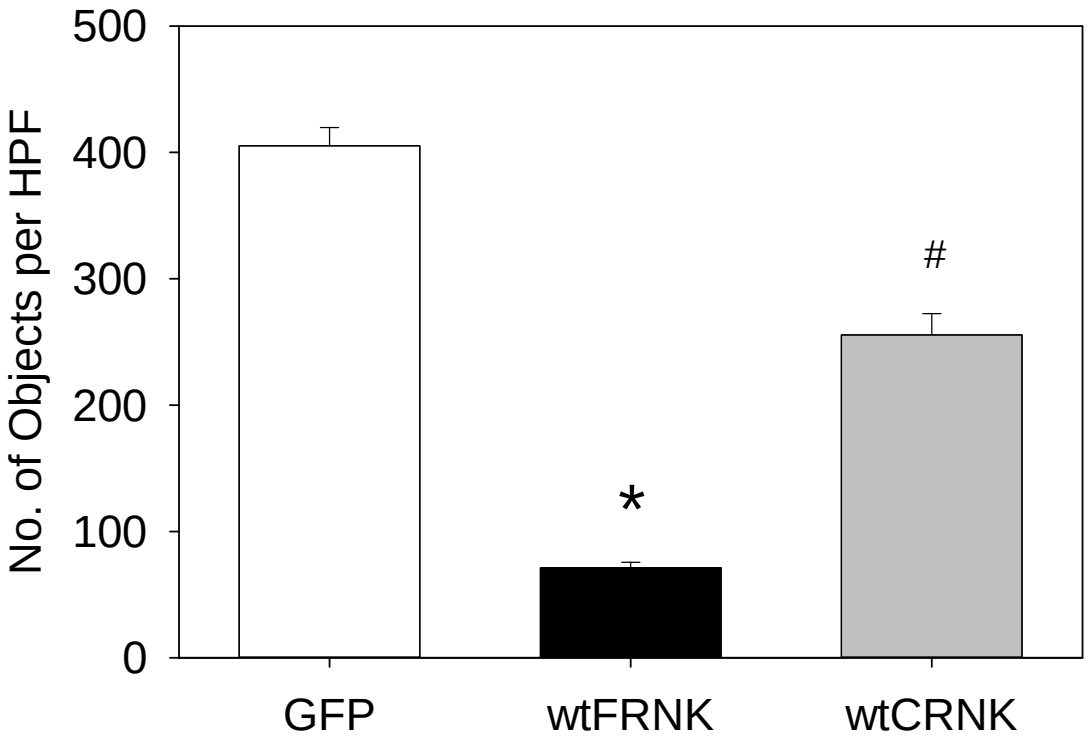

Supplemental Figure III

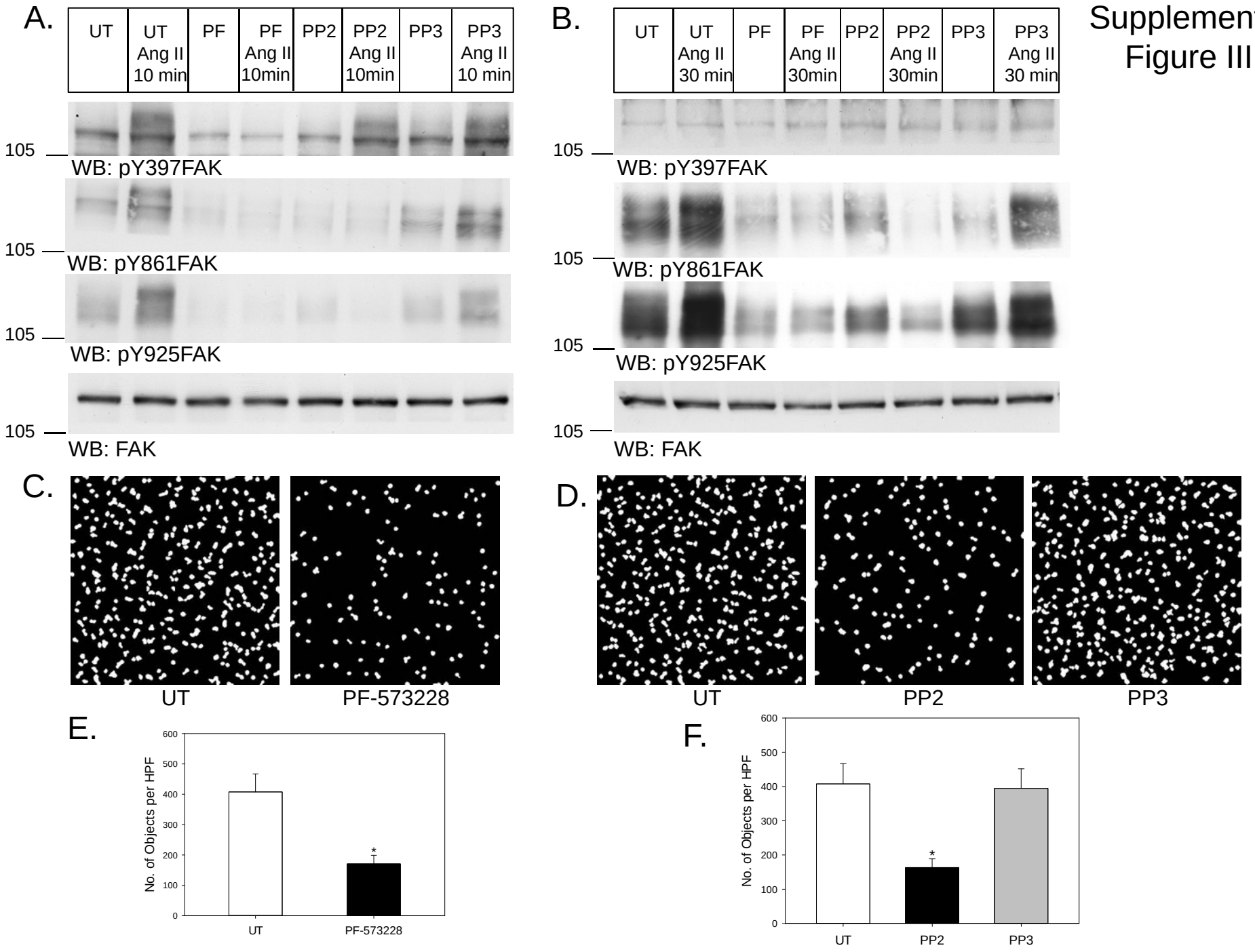

Supplemental Figure IV

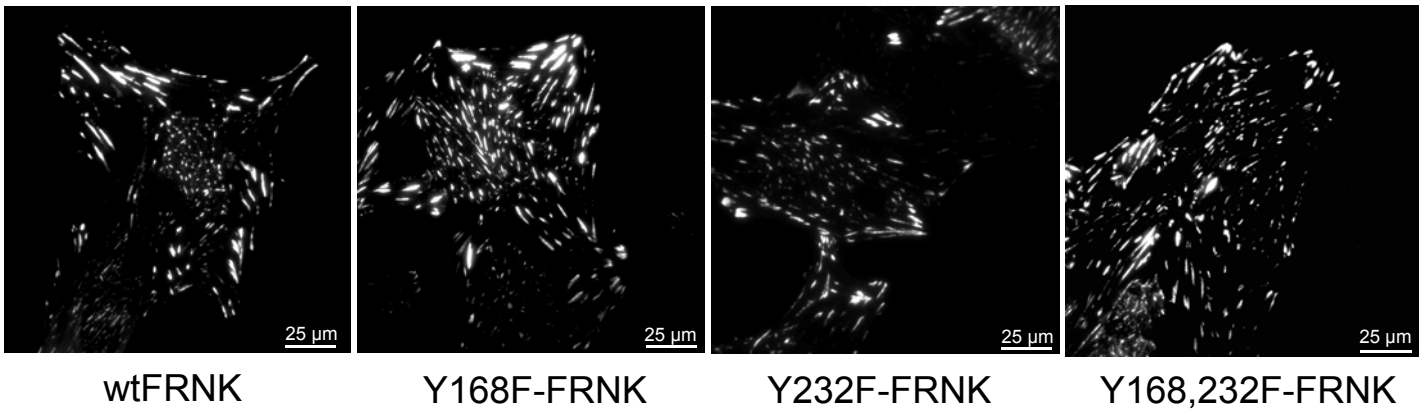

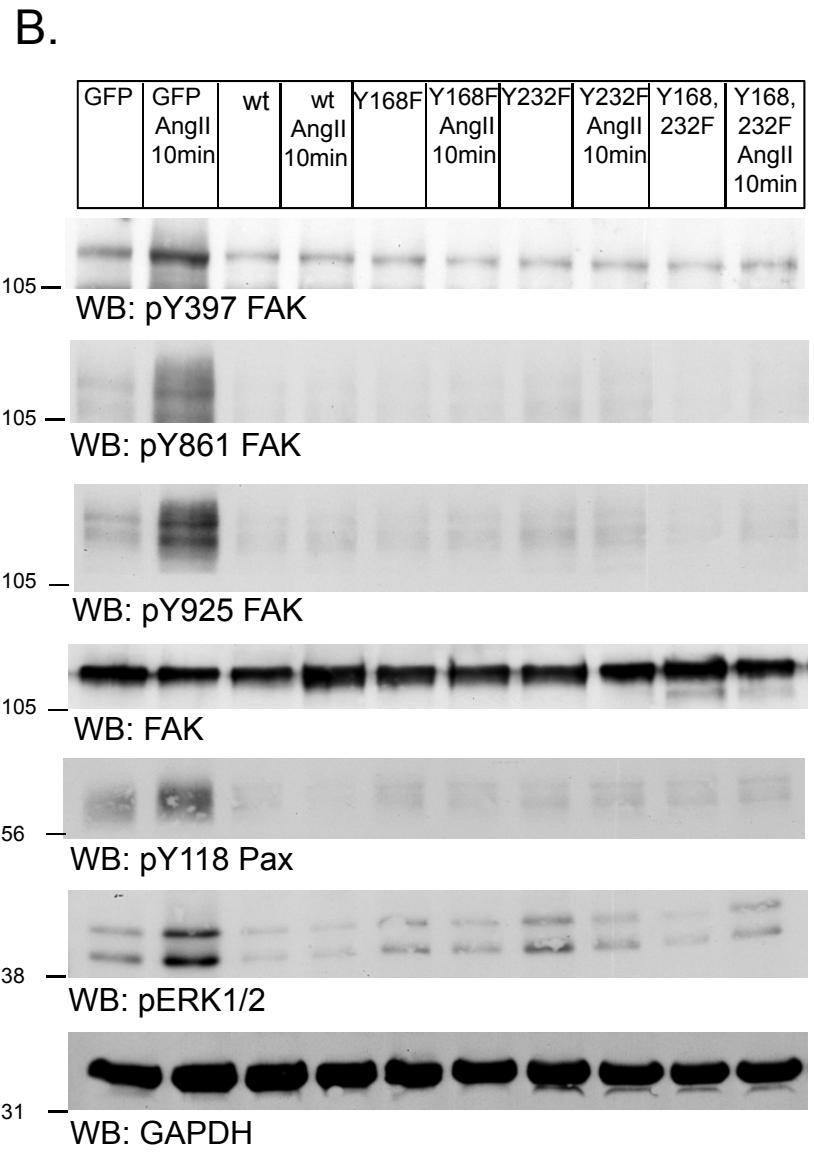

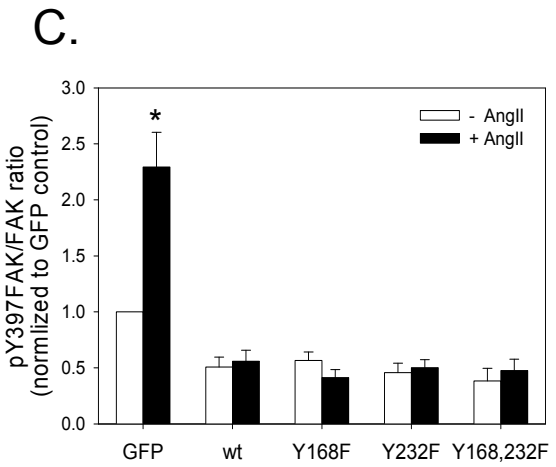

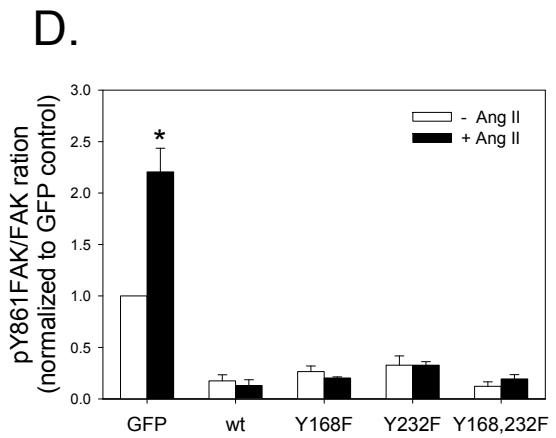

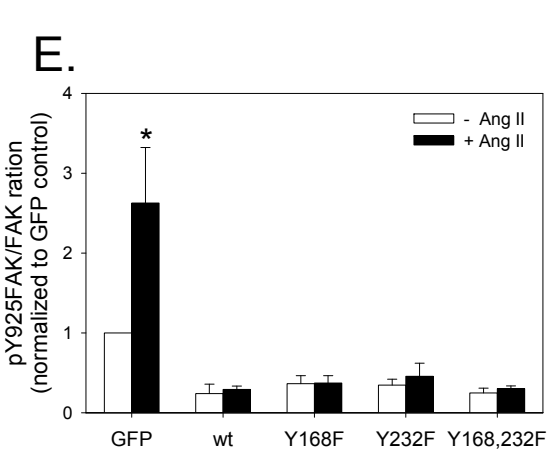

Supplemental Figure V

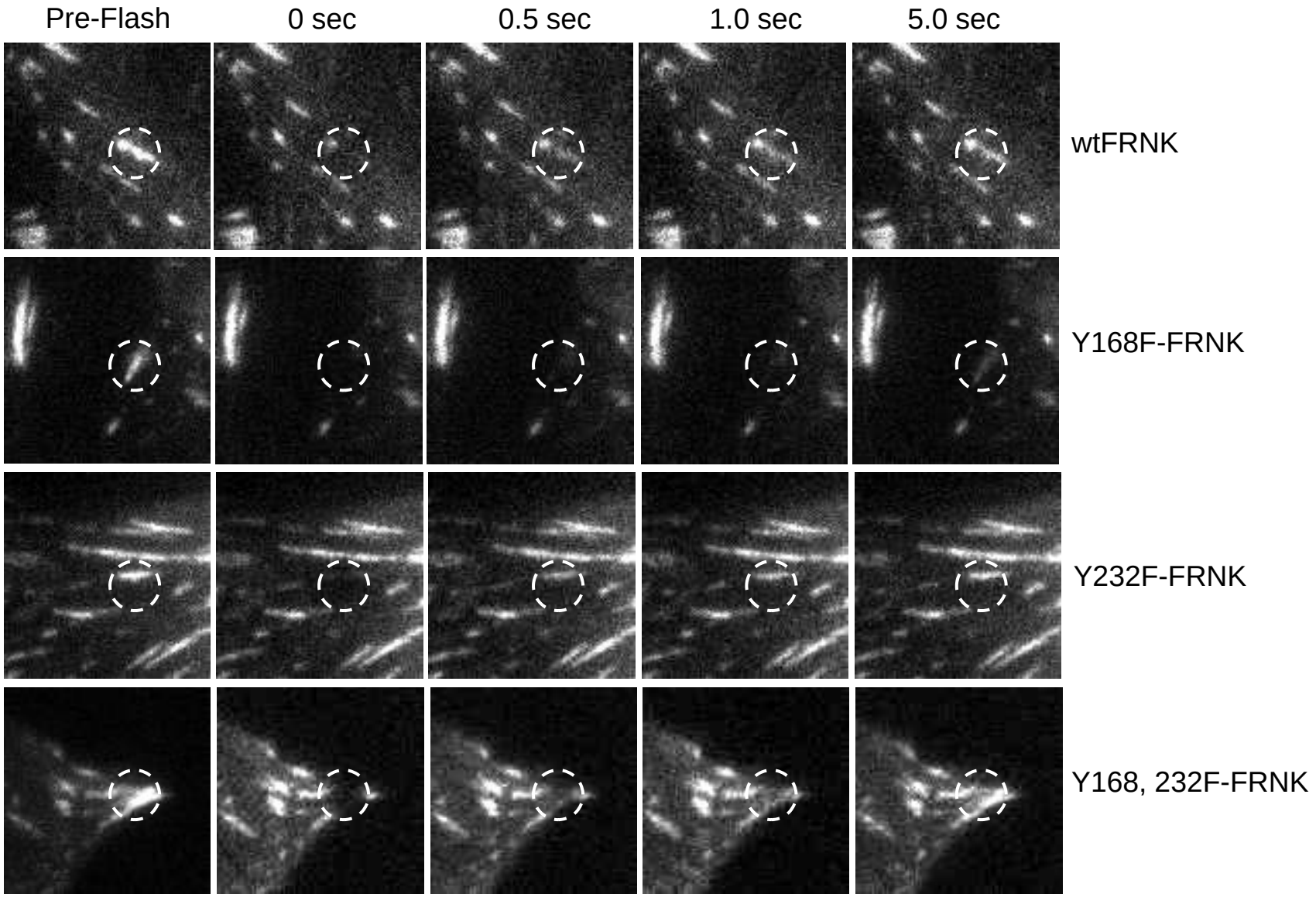

Supplemental Figure VI-A

60’ cell spreading on Fibronectin

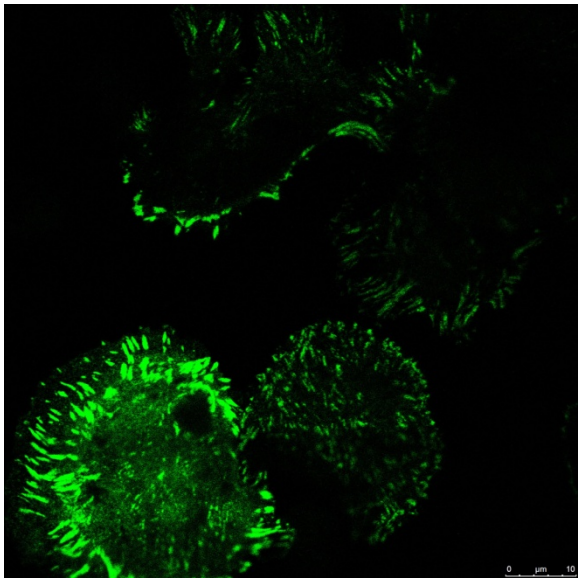
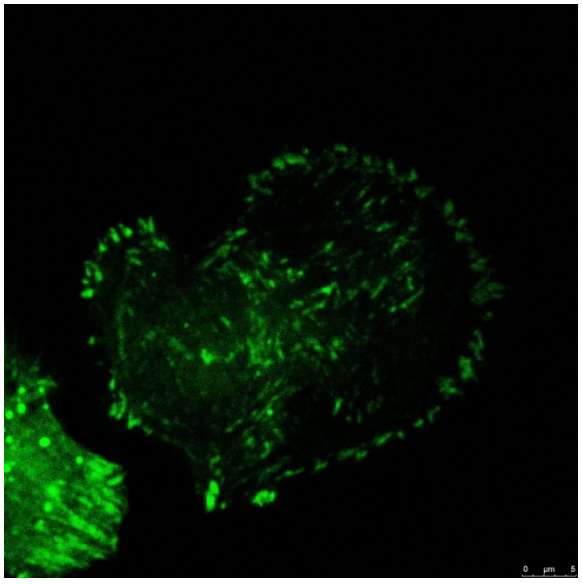

GFP

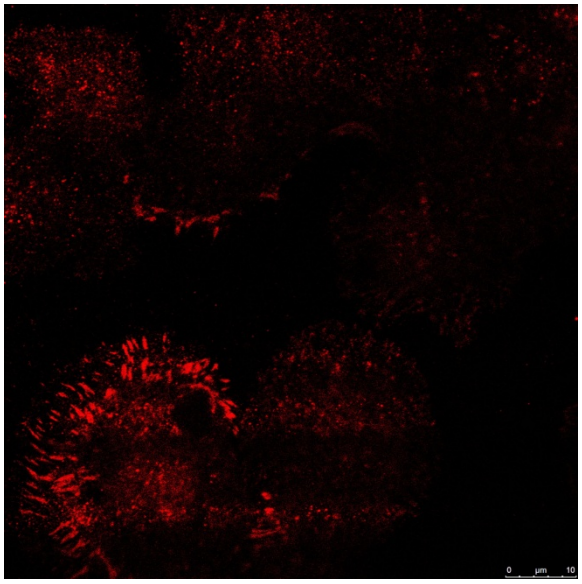
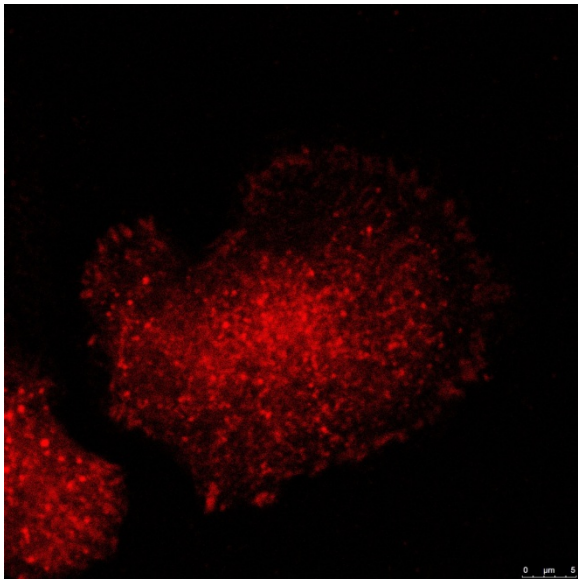

p130^{Cas}

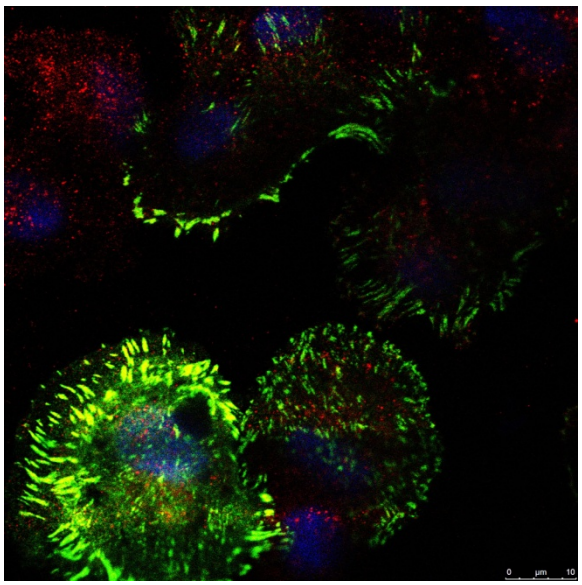
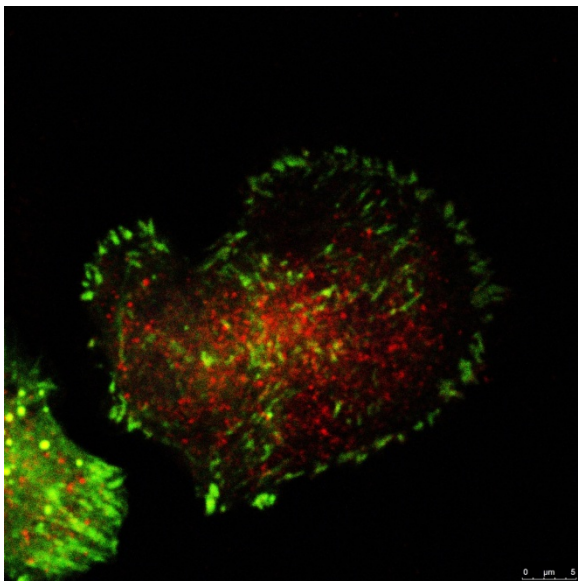

Merged

Adv-GFP-wtFRNK

Adv-GFP-Y168F-FRNK

Supplemental Figure VI-B

60’ cell spreading on Fibronectin

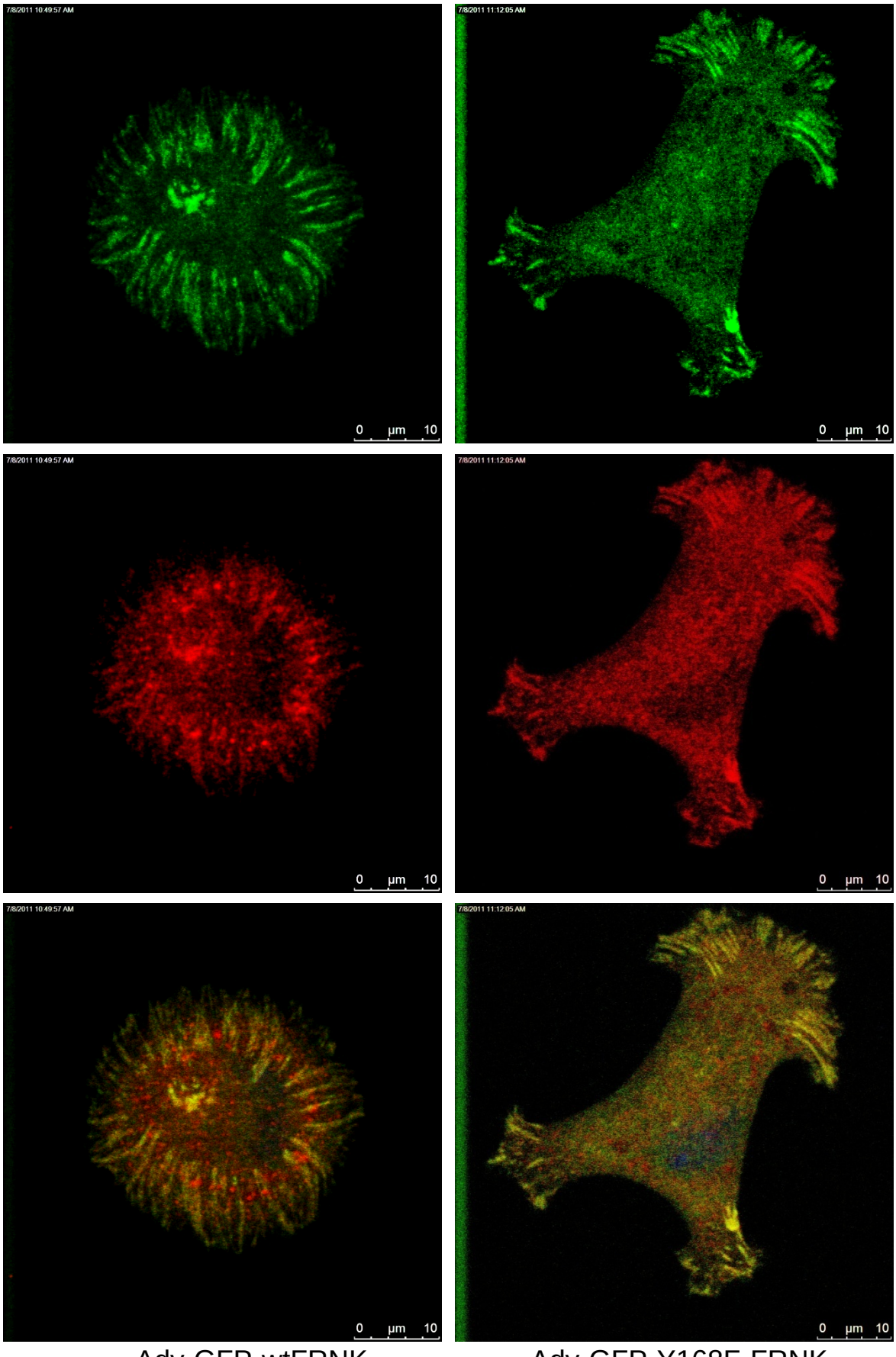

A.

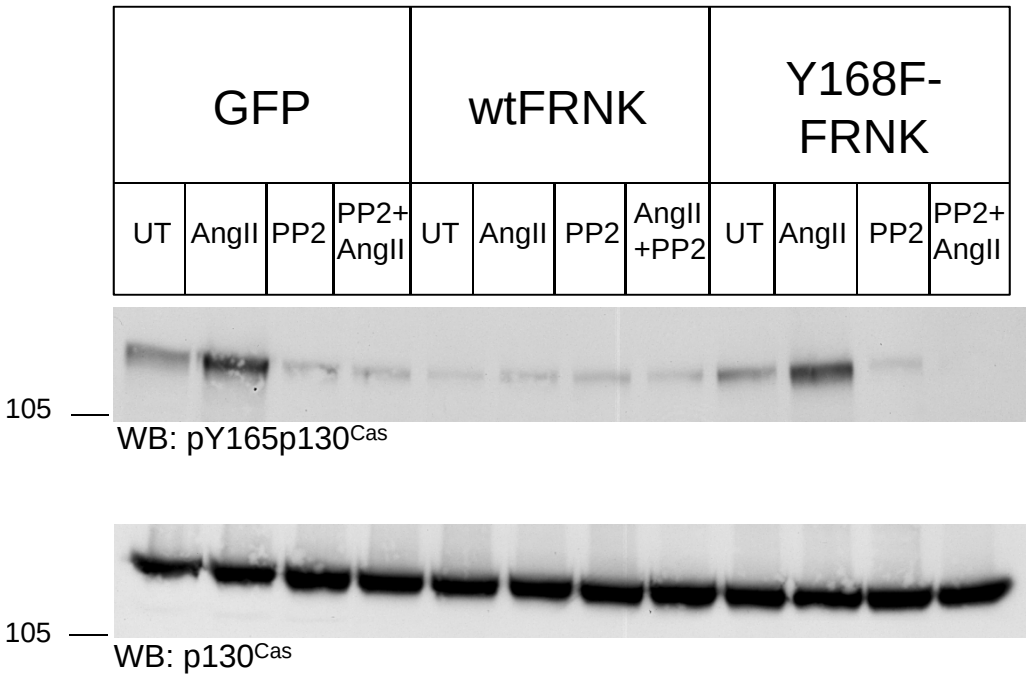

B.

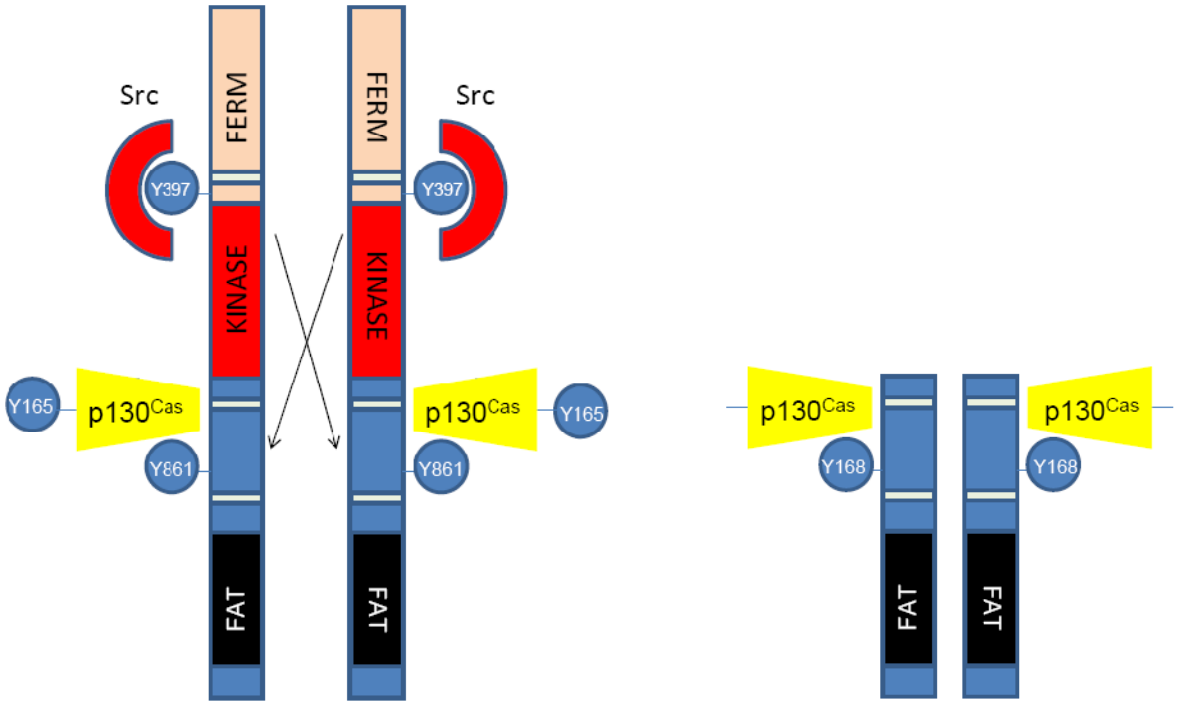

A. wtFAK

B. wtFRNK